International Journal of Robotics and Control Systems
Vol. 5, No. 3, 2025, pp. 1719-1742
ISSN 2775-2658
http://pubs2.ascee.org/index.php/ijrcs

Enhanced Fault Tolerant Control for Double Fed Asynchronous Motor Drives in Electric Vehicles

Toufik Roubache [a,c,1,*], Imad Merzouk [b,2], Souad Chaouch [c,3]

[a] Department of Electrical Engineering, Faculty of Technology, M'sila University, University Pole, Road Bourdj Bou Arreiridj, M'sila 28000, Algeria
[b] Applied Automation and Industrial Diagnostics Laboratory (LAADl), Faculty of Sciences and Technology, Djelfa University, PO Box 3117, Djelfa 17000, Algeria
[c] LSP-IE, Department of Electrical Engineering, Batna 2 University, 05078, Batna 5000, Algeria
[1] toufik.roubache@univ-msila.dz; [2] i.merzouk@univ-djelfa.dz; [3] s.chaouch@univ-batna2.dz
* Corresponding Author

ARTICLE INFO

Article history
Received May 08, 2025
Revised July 03, 2025
Accepted July 19, 2025

Keywords
Sensorless Fault Tolerant Control;
Robust Control;
Adaptive Neuro-Fuzzy Inference System;
Double Fed Asynchronous Motor;
Electric Vehicle

ABSTRACT

In the dynamic realm of electrical system traction, when Electric Vehicles (EVs) operate at various speeds or require high levels of accuracy and reliability in propulsion, malfunctions or faults might occur. Therefore, the drive system must be capable of detecting, estimating, and accommodating these faults using the designed controllers. This paper proposes an efficient Fault-Tolerant Control (FTC) based on the Adaptive Neuro-Fuzzy Inference System (ANFIS) and an integrated Luenberger Observer (LO) for speed tracking control of an EV driven by a Double-Fed Asynchronous Motor (DFAM). The ANFIS controller and LO are employed to play two functions: One for sensorless control and the other for estimating the fault that affect the machine. The performance metrics and accuracy of the ANFIS process are tested using statistical parameters, sush as Root Mean Square Error (RMSE), and convergence analysis. We use a High-Order Sliding Mode Controller (HOSMC), as a nominal control for DFAM. Moreover, the efficacy of the suggested control is demonstrated by comparing its performance with conventional FTC. We have found that ANFIS improves both the precision and responsiveness of the FTC, demonstrating no peak overshoot as well. The obtained results prove that the FTC-based on ANFIS was more enhanced fault estimation accuracy, reduced error, and faster convergence than the conventional FTC methods. Finally, these significant improvments underscore the effectiveness of the suggested algorithm.

1. Introduction

Nowadays, one of the most promising alternatives to traditional vehicles is Electric Vehicles (EVs). They represent a key application in which propulsion control relies on the availability and quality of Electric Machine Drive (EMD). The EMD plays a pivotal role in making vehicles, where different kinds of electric machines are broadly employed each delivering particular pros, selecting the most appropriate motor is based on a lot of criteria, mainly: wide torque–speed capability, high power and torque densities, high efficiency in wide torque–speed ranges, high reliability, and robustness [1], [2]. Table 1 illustrates the benefits and drowbacks of various types of electric

motors used in Evs [2]-[10]. According to the table, the Double-Fed Asynchronous Motor (DFAM) could be an adequate element for EV propulsion, which can attain twice the nominal power and rated torque, respectively [11], [12]. Additionally, several researchers have used this type of motor for EV applications, which is mentioned in [13]-[15].

Table 1. Characteristics of various motors used in EVs

No	Motors	Benefits	Drawbacks
1	BLDC Motor	- Accurate speed control - High reliability - High power density	- Require complex electronic control systems - Lack mechanical commutators - Expensive startup expenses
2	Asynchronous Motor	- Higher torque control - Straightforward construction - Cost effectiveness	- Limited speed - variation capabilities
3	Permanent Magnet Synchronous Motor	- High power density - Higher efficiency - Dynamic speed control possible	- More expensive due to permanent magnet - Difficult speed control - Narrow constant power region
4	Switched Reluctance Motor	- Powerful torque control - Robustness and reliability - Low manufacturing cost	- Vibration and noise - Higher torque ripple
5	Double Fed-Asynchronous Motor	- Cost-effectiveness - High power density - Robustness	- Limited uses - Sensitive to grid faults - Limitation of the rotor voltage

On the other hand, the DFAM is susceptible to various possible risks, which might occur from electrical and/or mechanical faults. These faults could result in substantial repercussions, including diminished product quality, and the motor can be compromised or interrupted. Consequently, the controllers may be unable to deliver appropriate control actions for the EV propulsion system [16], [17]. Therefore, the development of a solid fault tolerant control (FTC) and a monitoring system is crucial. To overcome these issues, sensorless FTC schemes have been developed using Adaptive Neuro-Fuzzy Inference System (ANFIS) to estimate these faults.

These methods aim to simplify the system architecture, fast fault detection, and enhance reliability FTC, particularly in handling motor faults in EV systems, ensuring a stable and efficient operation. In [18], the authors prove a new FTC scheme for distributed drive EV, employing a Co-simulation of Carsim and Matlab. This method can effectively improve the driving stability of the vehicle in different failure situations. However, there is a lack of thorough comparison with existing methods. Despite these issues, the study offers promising advancements in driving stability while ensuring efficient control in different cases of motor failure. The robust and fail-safe controller proposed in the paper [19] aims to ensure continued vehicle safety, even in the face of multiple failure scenarios. Simulations and actual industrial settings have been used to evaluate this approach, and the outcomes of the experiment demonstrate its efficacy. Furthermore, there is a lack of comparative studies with different methodologies and a lack of experimental investigation into the effects of flaws. In the event of a real-time motor breakdown, the reference [20] presents an active FTC strategy for EVs with an unscented Kalman filter observer.

The vehicle's dependability and safety can be successfully increased with this technique. On the other hand, because the influence of the suspension mechanism is not completely addressed in the research, this proposal is less efficient. In [21], the authors present a brake allocation method and a robust FTC for autonomous vehicle path following, taking into account the effects of braking actuator failures during the controller design process.

An experimental investigation using the Car-sim/Simulink and HIL systems validates the FTC. By doing this, the longitudinal dynamics of the vehicle are eliminated, and only the impact of braking actuator failures on the lateral dynamics of the vehicle is studied. An innovative FTC approach was introduced in [22], with a special emphasis on internal errors in the winding of switching reluctance motors (SRMs) used in electric vehicle applications. In order to enhance the output torque profile, the authors suggest a new FTC approach based on the average torque control

algorithm that incorporates a current compensation method. By accepting inherent flaws in SRMs and satisfying EV requirements, such as limiting torque ripples to reduce vibrations and acoustic noise and optimizing output torque, this technique improves vehicle acceleration and overall efficiency. A theoretical model with simulation validation and a comparison with a healthy model are the main topics of the paper. Conversely, the writers fail to include more comparison research using different methodologies.

This method's shortcomings include its sensitivity to changes in machine parameters, particularly in the case of open loop FTC. The recommended method in [23] addresses EV design and control, and it does so without relying on observer equations by efficiently applying passivity and the cascade of the vehicle-to-grid (V2G) system to create control laws. The asymptotic stability of the V2G system under the typical fault, which is Lock in Place (LIP) is not discussed in this research, which might improve this investigation. An extended Kalman filter (EKF) observer is used in the reference [24] to demonstrate a unique FTC of wye-connected 3-phase induction motor drives based on the Direct Field-Oriented Control (DFOC) technique. Results from experiments and simulations conducted under various operating settings are contrasted. Through this kind of fault, this technique showed a significant improvement in speed and torque pulsations. Although the method improves reliability and lessens the impact of faults, there are still a few things that may be done better. The sensitivity of the DFOC to parameter changes, such as variations in rotor or stator resistance, is not covered, nor is the intricacy and processing requirements of implementing EKF and DFOC in real-time.

Despite several drawbacks, the approach has potential for lowering hardware complexity and enhancing FTC dependability. To limit fluctuating torque and enhance the dynamic performance of a five-phase permanent magnet synchronous motor with an open circuit fault, the authors of [25] introduce a novel fault-tolerant direct torque and flux control (DFTC) technique. The novel aspect of the suggested approach is the use of DTFC, which employs stator flux orientation in the event of an open-circuit fault, in conjunction with the carrier-based pulse width modulation methodology to suppress third harmonic current. Through simulations and real-world application, the FTC performance was confirmed. The FTC approach for four-wheel motor drive EVs is proposed in the study [26], taking into account both motor power consumption and vehicle stability. Two levels make up the control structure in this study: a fault-tolerant coordinated controller at the bottom and a nonlinear model-predictive controller at the top. Numerical experiments are used to evaluate the effectiveness of the suggested control method. This innovative FTC technique lowers power usage while simultaneously enhancing driver comfort and vehicle stability.

FTC for a multiphase brushless direct current (BLDC) motor in an electric propulsion system is presented in the article [27]. The suggested approach is predicated on a comparison of three FTC approaches (minimum double phase, half phase, and many phases). Hardware-in-the-loop simulation of a 12-phase BLDC motor was used to validate the proposed FTC approaches.

Fast fault detection and highly reliable FTC of EVs are among the hottest topics in present study, according the most recent pertinent references. According to earlier research on EV fault tolerant control, the FTC controller by itself is unable to guarantee the required dynamic performance and function well in a range of EV circumstances.

However, one of the biggest obstacles to EV motor failure is choosing the right FTC technique. ANFIS and FTC together are still used in a number of newly released research studies, despite the availability of several sophisticated estimating techniques. ANFIS have drawn particular attention because of its low cost, quick convergence rate, and defect detection time.

In actuality, the ANFIS controller, one of the methods created to integrate the benefits of artificial neural networks (ANNs) and fuzzy logic control (FLC) [28], has been effectively used in numerous control applications. In order to control DFIM, an improved direct torque control (DTC) based on ANFIS was suggested by [28]. This method uses an ANFIS regulator to reduce the DFIM drive's torque, flux, and THD variations. When compared to the traditional method, this study shows how effective and efficient the 24 sectors DTC-ANFIS is. Using structural analysis, the

research suggests a fault diagnosis technique that makes use of Takagi Sugeno (TS) observers. Based on data-driven methods and the TS Zonotopic observer, the authors have proposed a hybrid strategy to identify and isolate defects in wind turbine systems.

A multioutput ANFIS was being used to identify the WT model. The approach is put into practice on a WT Benchmark in a realistic setting with several fault scenarios. A technique for managing brushless direct current (BLDC) was presented in [29]. It uses a fuzzy inference system based on an advanced adaptive network (AANFIS) to identify faults, including open circuit (OC) and short-circuit (SC) problems. The accuracy and power loss of current ANN approaches are compared in this study. Consequently, the combination of fuzzy logic and neural networks yields superior performance and great accuracy when compared to traditional networks.

Furthermore, the suggested method enhances the artificial neural network's accuracy and energy loss ratio. The performance of three sophisticated optimization algorithms: sunflower optimization (SFO), Jaya optimization algorithm (JOA), and black hole optimization (BHO) is examined by the authors of [30]. These are taken into consideration for improving defense against enemy attacks of the X-15 adaptive flight control systems (AFCS) and maximizing gains for a fractional order proportional integral derivative (FOPID) controller. A thorough assessment and accurate analysis validate the proposed methodology. The suggested approach aims to improve the accuracy and scalability of the system when managing voltage and current sensors. Random reinforcement learning processes may produce difficult convergences, such a deep deterministic policy gradient. Furthermore, these algorithms need to be thoroughly tested in a variety of AFCS motion scenarios in order to significantly increase the reliability of this approach. It is also important to consider that the controller might need to be re-tuned frequently in order to modify its gains in response to modifications in the system model. In order to address these problems, the work of [31] created a novel technique based on a significant level to use optimization algorithms like BHO, JOA, and SFO to find the ideal value of FOPID gains.

For navigating the maze-like world of optimization complexity, particularly in AFCS motion scenarios, this method offers a compass. In [32], the authors presented a novel method for the nonlinear system, specifically for Unmanned Aerial Vehicles (UAVs) traversing challenging terrain. The goal of this approach was to integrate the FOPID with Time Invariant Derivative (FOPID-TID) controller with the Hybrid Archimedes Optimization Algorithm-Rider Optimization Algorithm (HAOAROA). The latter was used in conjunction with a fractional calculus to improve robustness and stability. The suggested method maintains UAV control precision and trajectory smoothness while adapting to shifting environmental variables. The authors of [33] suggest a novel method for Automatic Voltage Regulation (AVR) that combines ANFIS with a Hybrid Intelligent Fractional Order Proportional Derivative2+Integral (FOPDD+I) controller. The comparison of three scenarios: the AVR system without a controller, with a traditional PID controller, and with the recommended method is where the novelty lies. Effective performance metrics, including rise time, settling time, overshoot, and steady-state error, were found using this method for the FOOD+I-ANFIS strategy in AVR. The control of the 3-DOF Helicopter System is covered in the paper [34], which successfully uses three cutting-edge AI techniques to design control laws based on tuning a FOPID controller: Harris Hawks Optimization (HHO), Hybrid Sperm Swarm Optimization Gravitational Search Algorithm (HSSOGSA), and Hybrid Grey Wolf Optimization Particle Swarm Optimization (HGWOPSO).

After comparing the suggested approach to these three algorithms, it is shown that the HHO algorithm improves flight dynamics, stability, and dynamic reaction. The disadvantage of the proposed method is that it solely depends on simulations with little insight into the algorithms being employed. In order to offer recommendations on boosting efficacy, the authors' study in [35] focuses on the causes, problems, and limitations of UAV technology as well as Chinese remedies to these problems. In order to get precise predictions that go beyond experimental observations, they have applied the Simple Iterative Method for Pressure Linked Equations (SIMPLE) algorithm to UAV rotor systems. However, the battery's restricted power source is the main disadvantage of UAVs. The authors proposed a solution to address this problem, demonstrating that meta heuristic

algorithms are a popular optimization strategy for resolving UAV path planning issues with one or more objectives. The authors further demonstrate that the COA is one meta heuristic technique that has demonstrated exceptional promise in handling nonlinear optimization issues.

Currently, most researchers design Fault Tolerance Control (FTC) schemes by constructing observers. In [36] a new FTC scheme for dual three-phase induction machine based EV was introduced, employing a sliding mode observer approach. While the approach reduces faults and enhances reliability, several area need enhancement. The authors in [37] present an adaptive observer-based FTC scheme for wind turbines. The simulation results demonstrate that the FAFE algorithm's proposed FTC strategy effectively stabilizes the defective system and outperforms the baseline on the WT benchmark model. In [38], the authors proposed a robust actuator fault reconstruction for Takagi-Sugeno (T-S) fuzzy systems, and they have used a Fuzzy Synthesized Learning and Luenberger Observer. To illustrate the efficacy of the suggested methods, a numerical example and a simulation are given by them.

In order to overcome the issues with malfunctioning control systems, recent research has demonstrated the significance of incorporating sophisticated control algorithms based on FTC in EV systems. Therefore, a combination of sensorless FTC and ANFIS is needed to produce effective motor control and ensure performance in vehicle [39]-[42]. This requirement has prompted the development of innovative EV monitoring and control systems, where cutting-edge technologies based on neuro-fuzzy systems have grown in significance [43]-[47].

This paper seeks to develop a strong and straightforward control strategy for DFAM control by integrating FTC and ANFIS. The goal of our suggested method is to make performance resilient to uncertainties as well as external disruptions. This comprises excellent control of the EV. The research contribution can be clarified as follows:

- A development of an FTC method based on ANFIS with LO to improve the performance of DFAMs drives in EVs applications.
- A sensorless control based on LO is designed to improve estimation accuracy under fault conditions. Furthermore, it guarantees finite-time convergence and robustness against faults affecting the motor.

The suggested study is structured into six sections: Section 2 introduces the dynamic model of EV propulsion system, while Section 3 addresses the conventional sensorless FTC strategy. Section 4 provides more details about the mechanism by which the proposed ANFIS functions. The simulation results, which demonstrate the comparison between the suggested ANFIS-FTC and the conventional FTC methods, are illustrated in Section 5. At last, Section 6 addresses the conclusion and outlines potential future research.

2. Complete System Mathematical Modeling

The modeling of propulsion systems has a vital role in EVs transitioning energy, where these systems transform the mechanical energy of motors into the wheels of vehicle. The dynamic modeling of EV specializes in the interaction between the vehicle and external disturbances to create resistant forces that apply load torque in the drive rotor.

2.1. Modeling of Electric Vehicle

Fig. 1 depicts the two main areas where EVs generally operate: constant torque and constant power. In the constant torque range, the motor delivers maximum torque from standstill to base speed, allowing powerful acceleration and climbing. Beyond the base speed, the motor shifts to the constant power area, where it maintains maximum power output by reducing torque as speed increases. This allows higher top speed [3]. The dynamic model for vehicle is represented by the following equation [48]:

$$F_t = \frac{1}{2}\rho C_a S_f (V_v \pm V_w)^2 \pm M_v g \sin(\alpha_p) + C_r M_v g + M_v \dot{V}_v \quad (1)$$

Where F_t is the total force exerted on the vehicle in motion, ρ is air density, C_r, C_a are rolling and aerodynamic coefficient, M_v, S_f, V_w, and V_v are the mass, frontal area, wind speed, and velocity of EV, respectively.

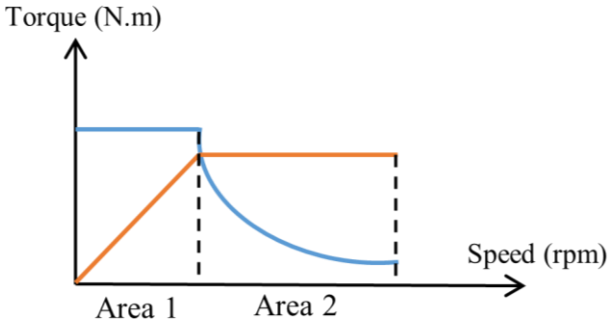

Fig. 1. Mechanical characteristics of an EV

2.2. Faulty Model of DFAM

The DFAM mathematical model in the αβ stationary reference frame inserting the fault.

$$\begin{cases} i_{\alpha s} = -\lambda i_{\alpha s} + \dfrac{k}{T_r}\varphi_{\alpha r} + k w_r \varphi_{\beta r} - k v_{\alpha r} + b_1 v_{\alpha s} + f_{\alpha s} \\ i_{\beta s} = -\lambda i_{\beta s} + \dfrac{k}{T_r}\varphi_{\beta r} + k w_r \varphi_{\alpha r} - k v_{\beta r} + b_2 v_{\beta s} + f_{\beta s} \\ \dot{\varphi}_{\alpha r} = \dfrac{L_m}{T_r} i_{\alpha s} - \dfrac{\varphi_{\alpha r}}{T_r} + w_r \varphi_{\beta r} + v_{\alpha r} \\ \dot{\varphi}_{\beta r} = \dfrac{L_m}{T_r} i_{\beta s} - \dfrac{\varphi_{\beta r}}{T_r} - w_r \varphi_{\alpha r} + v_{\beta r} \end{cases} \quad (2)$$

Where: $f_{\alpha s}$ and $f_{\beta s}$ are the input additive faults.

Therefore, the system input that is subject to additive faults is described by [36]:

$$\begin{cases} f_{\alpha s} = A sin(w_i + \varphi) \\ f_{\beta s} = A cos(w_i + \varphi) \\ w_i = 2\pi f_i \end{cases} \quad (3)$$

Where A and φ are the amplitude and phase, respectively. f_i is a specific frequency that will be utilized to identify faults caused by rotor and stator asymmetries as follows [36]:

$$f_i = \left(1 \pm 2k \frac{s_w}{w_s}\right) f_s \quad (4)$$

With: $s_w = w_s - p w_r$ is the slip angular frequency, w_s and f_s are stator angular and supply frequency, respectively, and k is a positive integer. In case of faulty model, the stator mechanical faults are added to (2).

Where:

$$\begin{cases} f_{\alpha s} = A\left[w_i cos(w_i t + \varphi) - \dfrac{1}{\tau_1} sin(w_i t + \varphi)\right] \\ f_{\beta s} = -A\left[w_i sin(w_i t + \varphi) + \dfrac{1}{\tau_2} cos(w_i t + \varphi)\right] \\ \tau_1 = \tau_2 = \dfrac{\sigma L_m}{R_s} \end{cases} \quad (5)$$

The mechanical drive is given by:

$$\begin{cases} J_t \dot{w}_r = T_e - T_l - B_x w_r \\ T_e = p\left(\varphi_{\alpha r} i_{\beta s} - \varphi_{\beta r} i_{\alpha s}\right) \end{cases} \quad (6)$$

Where: J_t, T_e, T_l and B_x are the total coefficient inertia, motor torque, load torque, and friction coefficient, respectively, $\varphi_{\alpha r}$ and $\varphi_{\beta r}$ are the rotor flux.

3. Sensorless HOSMC Strategy

A fault tolerant control system automatically manages system failures while maintaining stability and performance during such events. Fig. 2 depicts the proposed adaptable design for FTC that ensures maximum performance while keeping the overall system failure rate to an acceptable level. This strategy significantly enhances the reliability of the driving system.

The SMC is a form of variable structure control that is both efficient and reliable for nonlinear and linear systems. The primary role of SMC is to supply a switching surface that complies with the principles of existence, convergence, and stability. The desired state can be attained from the switching surface, via suitable path adjustments to the control system's structure. Consequently, the design of a SMC involves two crucial stages: First, designing a sliding surface, second, setting a control law to attract the state trajectory to the surface [49]. Therefore, the surface must meet the criteria for convergence and stability. On the other hand, SMC has an undesirable effect known as the chattering phenomenon, which arises from the discontinuous state of its control actions. To overcome this disadvantage, it is necessary to find an efficient controller. In this study, we have selected the HOSMC based on the super-twisting algorithm (STA), because it achieves robust control to mitigate this issue [50]-[52]. The sliding surface can be defined as follows [53]:

$$S(x) = \left(\frac{d}{dt} + \lambda\right)^{n-1} e(x) \quad (7)$$

With λ is a positive coefficient, n is the system order, and $e(x)$ is the tracking error vector. First, to select the attractiveness condition, we should take into account the Lyapunov function as follows:

$$V(s) = \frac{1}{2} S^2 \quad (8)$$

As a necessary and sufficient condition, the time derivative of (8) must be negative [54]:

$$\dot{S}S < 0 \quad (9)$$

Second, to obtain the equivalent control, we must consider the following conditions for the invariance of the surface: $\dot{S} = S = 0$ [55]. Therefore, a nonlinear term must be added to the equivalent control to achieve the total control, which provides a convergence and a sliding regime as follows [56]-[58]:

$$\begin{cases} u = u_n + u_e \\ u_n = -\gamma sign(S) \end{cases} \quad (10)$$

With: γ is a positive constant.

By applying this control to the DFAM, we have introduced the following two sliding surfaces for speed and flux.

$$\begin{cases} S_1 = k_1\left(w_{ref} - w_r\right) + \left(\dot{w}_{ref} - \dot{w}_r\right) \\ S_2 = k_2\left(\Phi_{ref} - \Phi_r\right) + \left(\dot{\Phi}_{ref} - \dot{\Phi}_r\right) \end{cases} \quad (11)$$

With: k_1 and k_2 are positive gains

The first derivation of (11) is given by:

$$\begin{cases} \dot{S}_1 = k_1\left(\dot{w}_{ref} - \dot{w}_r\right) + \left(\ddot{w}_{ref} - \ddot{w}_r\right) \\ = k_1\left(\dot{w}_{ref} - \frac{1}{J}\left(-\frac{pL_m}{L_s}\left(i_{r\beta}\varphi_{r\alpha}\right) - k_f w_r - T_l\right)\right) + F_1 \\ \dot{S}_2 = k_2\left(\dot{\Phi}_{ref} - \dot{\Phi}_r\right) + \left(\ddot{\Phi}_{ref} - \ddot{\Phi}_r\right) \\ = k_2\left(\dot{\Phi}_{ref} - V_{r\alpha} + \frac{L_m}{T_r} i_{s\alpha} - \frac{1}{T_r}\varphi_{r\alpha}\right) + F_2 \end{cases} \tag{12}$$

Where:

$$\begin{cases} F_1 = \left(\ddot{w}_{ref} - \ddot{w}_r\right) \\ F_2 = \left(\ddot{\Phi}_{ref} - \ddot{\Phi}_r\right) \end{cases} \tag{13}$$

Hence, the STA suggested for this control contains two parts: continuous and discontinuous u_1, u_2, respectively [59], [60]:

$$u = u_1 + u_2 \tag{14}$$

With:

$$u_1 = \begin{cases} -\lambda |S_0|^{\Gamma} sign(S) \; if \; |u| > S_0 \\ -\lambda |S|^{\Gamma} sign(S) \; if \; |u| \le S_0 \end{cases} \tag{15}$$

$$u_2 = \begin{cases} -u & if \; |u| > U_M \\ -\gamma sign(S) & if \; |u| \le U_M \end{cases} \tag{16}$$

3.1. Luenberger Observer

The whole developed closed-loop system has been modeled, using a Luenberger observer (LO). The state equation can be constructed as follows:

$$\dot{\hat{x}}_{\alpha\beta} = A\hat{x}_{\alpha\beta} + Bu_{\alpha\beta} + L_o e_{\alpha\beta} \tag{17}$$

With L_O is the gain matrix of observer, which regulates the dynamics and the observer's robustness. It is determined as follows:

$$K_L = \begin{bmatrix} L_{o1} & L_{o2} & L_{o3} & L_{o4} \\ L_{o2} & -L_{o1} & L_{o4} & -L_{o3} \end{bmatrix}^T \tag{18}$$

The coefficients L_{o1}, L_{o2}, L_{o3}, and L_{o4} are defined as follows:

$$\begin{cases} L_{o1} = (k-1)\left[\frac{1}{\sigma L_s} + \frac{(1-\sigma)}{\sigma T_r} + \frac{1}{T_r}\right] \\ L_{o2} = (k-1)\hat{\omega}_r \\ L_{o3} = \frac{(1-k^2)}{\delta}\left[\frac{1}{\sigma L_s} + \frac{(1-\sigma)}{\sigma T_r} + \frac{1}{T_r}\right] + \frac{(k-1)}{\delta}\left[\frac{1}{\sigma L_s} + \frac{(1-\sigma)}{\sigma T_r} + \frac{1}{T_r}\right] \\ L_{o4} = \frac{(k-1)}{\delta}\hat{\omega}_r, k > 0, \sigma = 1 - \frac{{L_m}^2}{L_s L_r}, T_r = \frac{L_r}{R_r}, \delta = \frac{L_m}{L_s L_r \sigma} \end{cases}$$

Thus $e_{\alpha\beta}$ is the difference between actual and estimated outputs, which is defined as follows:

$$\begin{cases} e_{\alpha s} = [\hat{\imath}_{\alpha s} \quad - \quad i_{\alpha s}]^T \\ e_{\beta s} = [\hat{\imath}_{\beta s} \quad - \quad i_{\beta s}]^T \end{cases} \tag{19}$$

The estimated rotor speed is expressed as follows:

$$\hat{\omega}_r = K_p(e_{\alpha r}\hat{\varphi}_{r\beta} - e_{\beta r}\hat{\varphi}_{r\alpha}) + K_i \int (e_{\alpha r}\hat{\varphi}_{r\beta} - e_{\beta r}\hat{\varphi}_{r\alpha})dt \tag{20}$$

With $e_{\alpha r}$ and $e_{\beta r}$ are errors signals between the estimated and measured rotor flux. K_p and K_i are gains for proportional and integral signal, respectively.

4. Suggested ANFIS-FTC Method

The straightforward application of adaptive neural network technology in machine control has enabled the resolution of various issues related to fault tolerance. In this context, a conventional FTC system is replaced by a controller based on ANFIS, as illustrated in Fig. 2. Furthermore, by incorporating Fuzzy Logic into the control selection process, the results not only improve fault tolerance but also showcase the adaptability and effectiveness of this strategy in addressing complex system faults.

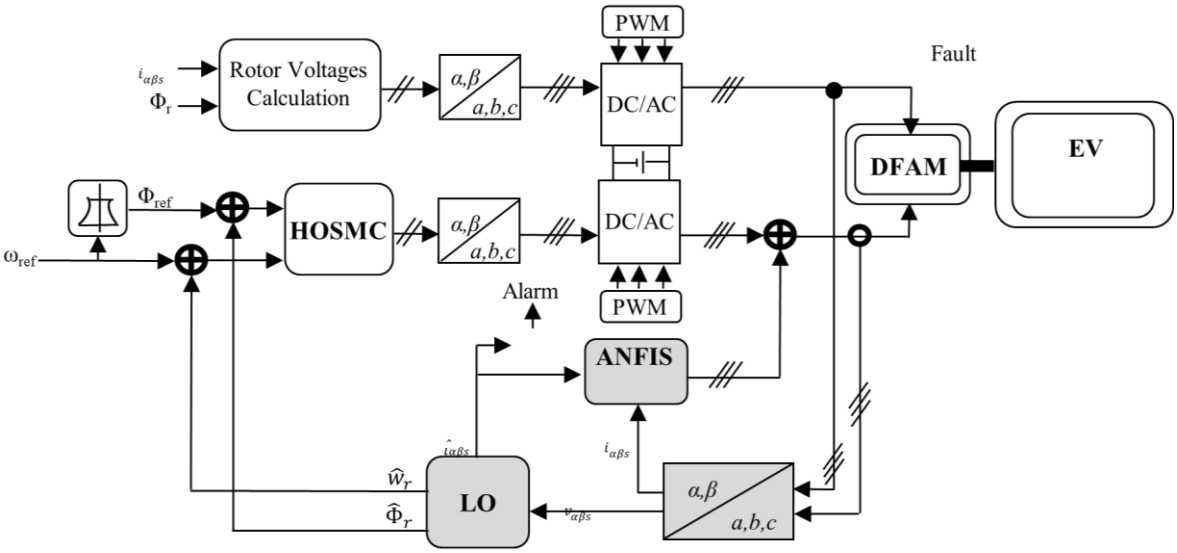

Fig. 2. Scheme of the proposed ANFIS-FTC for DFAM in the EV propulsion system

4.1. ANFIS Strategy

Currently, numerous applications of neuro-fuzzy systems have been developed for modeling and controling industrial systems [61]-[65]. Nevertheless, ANFIS allows the automatic generation of fuzzy rule-based models that utilize the Takagi-Sugeno inference model [66], [67]. The rule outputs are generated by a linear combination of input parameters and a constant term. The final outcome is obtained by averaging the weights outputs of all the rules [68]. ANFIS is an advanced mixture of an artificial neural network (ANN) and a fuzzy inference system (FIS) that provides a powerful and integrated solution to complicated engineering issues by capitalizing the strengths of both models [64], [69]. Fig. 3 shows the ANFIS design model, demonstrating how the ANFIS output estimates the fault from the DFAM drive, shown in (3). Fig. 4 shows the ANFIS fault tolerant method. In this case, ANFIS employs a five-layer neural network structure [70]-[76]:

Layer 1 is responsible for calculating two control inputs. The first control input, X_1 represents the error between the measured and estimated stator currents. The second input control, X_2 is calculated from the first derivative of X_1. Layer 2 involves the fuzzification of the output values from Layer 1. The membership function is modeled by the triangular function as:

$$Q_i^1 = h(x) \tag{21}$$

In Layer 3, neurons are utilized to calculate the normalized degrees of rule fulfillment. The equation which represents the output of this Layer is as follows:

$$Q_i^3 = \frac{w_i}{\sum_{k=1}^{2} w_k} \tag{22}$$

Layer 4 is responsible for the defuzzification of the first-order TS type fuzzy rules, which is performed to determine the weights total output. Node function is given by:

$$Q_i^4 = \tilde{w}_i f_{oi} = \tilde{w}_i (p_i X_1 + q_i X_2 + r_i) \tag{23}$$

Finally, in Layer 5, the output signal is computed using ANFIS, which uses in equation.

$$Q_i^5 = f = \sum_{i=1} \tilde{w}_i f_{oi} = \tilde{w}_i (p_i X_1 + q_i X_2 + r_i) \tag{24}$$

As clarified in Fig. 3, the ANFIS integrates the Fuzzy Inference System (FIS) mechanism within the structure of a Neural Network (NN). Additionally, the TS fuzzy model, which includes two inputs: X_1 and X_2, and a single output is considered. Typically, the TS fuzzy includes three rules, which are expressed as:

Rule I: if $X_1=A_1$ and $X_2=B_1$, then $f_{o1} = p_1 X_1+q_1 X_2 + r_1$

Rule II: if $X_1=A_2$ and $X_2=B_2$, then $f_{o2} = p_2 X_1+q_2 X_2 + r_2$

Rule III: if $X_1=A_3$ and $X_2=B_3$, then $f_{o3} = p_3 X_1+q_3 X_2 + r_3$

Where $f_{o1,2,3}$ are outputs signals, A_1, A_2, A_3, B_1, B_2, B_3 and p_1, p_2, p_3, q_1, q_2, q_3, r_1, r_2, r_3 are nonlinear and linear parameters, respectively.

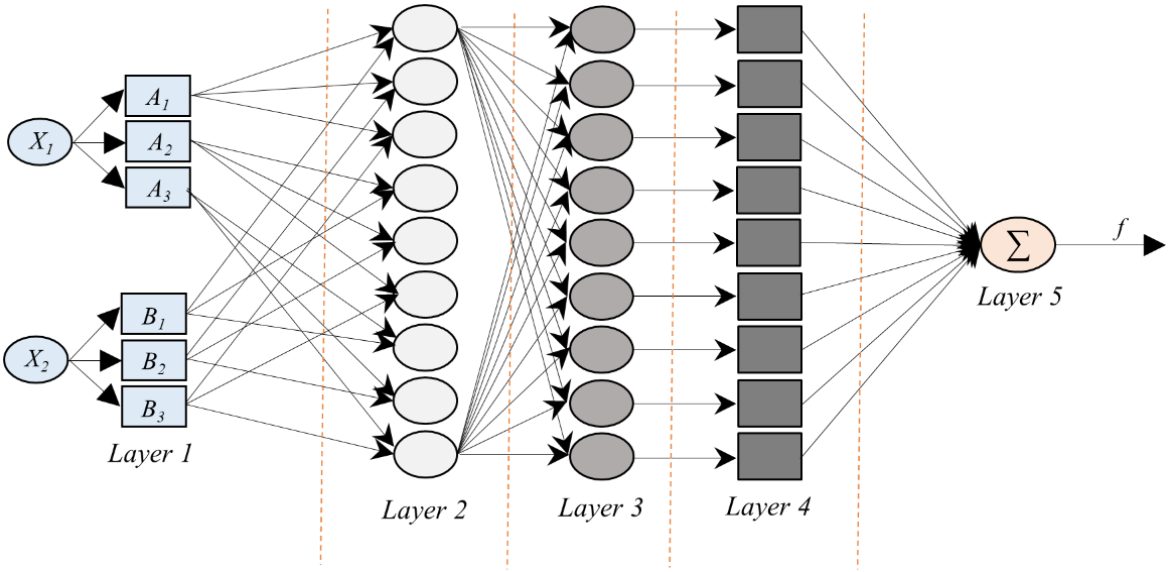

Fig. 3. Five layer ANFIS mechanism with two parameter inputs and one output

In this study, the ANFIS mechanism generates changes in the reference voltage based on the currents error X_1 and the derivate of the currents error X_2, are defined as:

$$\begin{cases} X_1(k) = i_{\alpha\beta s}(k) - \hat{\imath}_{\alpha\beta s}(k-1) \\ X_2(k) = \dfrac{d}{dt}\,(X_1(k)) \end{cases} \tag{25}$$

Where $i_{\alpha\beta s}$ and $\hat{\imath}_{\alpha\beta s}$ are the actual and estimated currents.

The ANFIS control output can expressed as follows:

$$U(k) = K_\beta(X_1(k) + X_2(k)) \tag{26}$$

Where, K_e, K_{de} *and* K_β are the inputs and output scaling factors.

The aim of this control strategy is to develop an ANFIS fault tolerant controller for the system described in (2). The ANFIS algorithm is employed to create a FTC system, specifically designed to enhance the performance of the system. In this work, the ANFIS structure contains two inputs and one output. The input of ANFIS is the output of residual signals training data of X_1 and X_2. The outcome of ANFIS is FTC of DFAM drive. The block diagram is shown in Fig. 4.

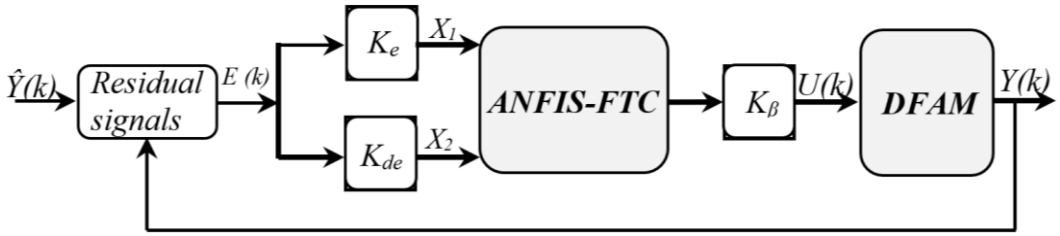

Fig. 4. Scheme of ANFIS-FTC controller

The suggested ANFIS controller's performance is demonstrated using essential metrics, such as root mean square error (RMSE), integral absolute error (IAE), and integral square error (ISE). These metrics will be summarized in a performance table. In this case, the standard performance indices can be expressed as follows [77]-[80]:

$$\begin{cases} RMSE = \sqrt{\dfrac{1}{n}\displaystyle\sum_{k=1}^{n} {e_k}^2} \\ ISE = \displaystyle\int_0^t {e_k}^2 dt \\ IAE = \displaystyle\int_0^t |e_k| dt \end{cases} \tag{27}$$

Where n denotes the dataset size

The network is trained for 100 epochs, with the target error set to a minimal value. Fig. 5 illustrates the training error waveform for the ANFIS controller, while Fig. 6 presents the ANFIS network model for this controller. The input membership function obtained after training, and it is shown in Fig. 7. The FIS is trained using neural networks' hybrid learning approach. The ANFIS controller's consequent and premise parameters are identified using the hybrid learning approach, which combines least square estimation and gradient descent. The FIS is well trained utilizing the neural network, with a minimum RMSE at 100 epochs. The FIS is generated using the grid partitioning technique, which consists of six trapezoidal membership functions. Table 2 summarizes the training parameters.

Table 2. ANFIS training

Training Parameters	Specific Details
Number of inputs	2
Number of outputs	1
Generate FIS	Grid partitioning
Number of Membership Functions	6
Membership Function Type	Trapezoidal
Number of Fuzzy Rules	9
Optimization method	Hybrid method

The advents of this method involve rapid tracking speed and high tracking accuracy.

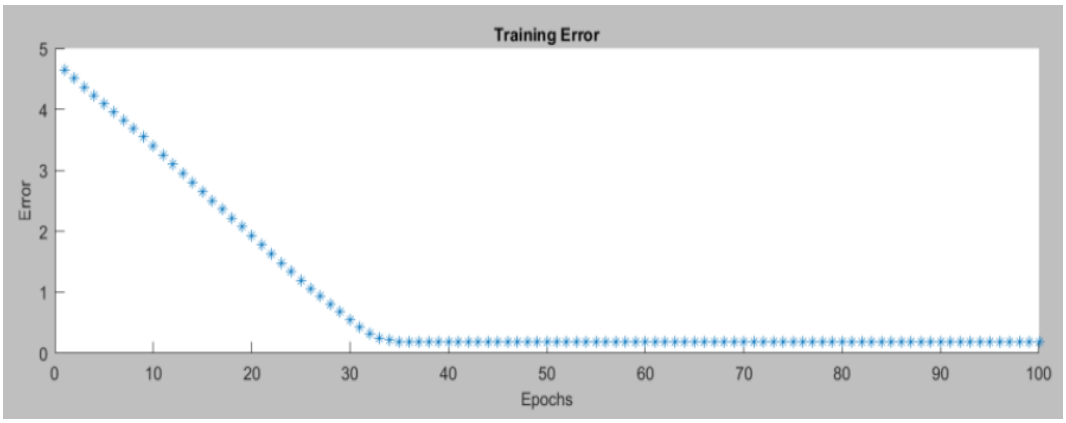

Fig. 5. Training error

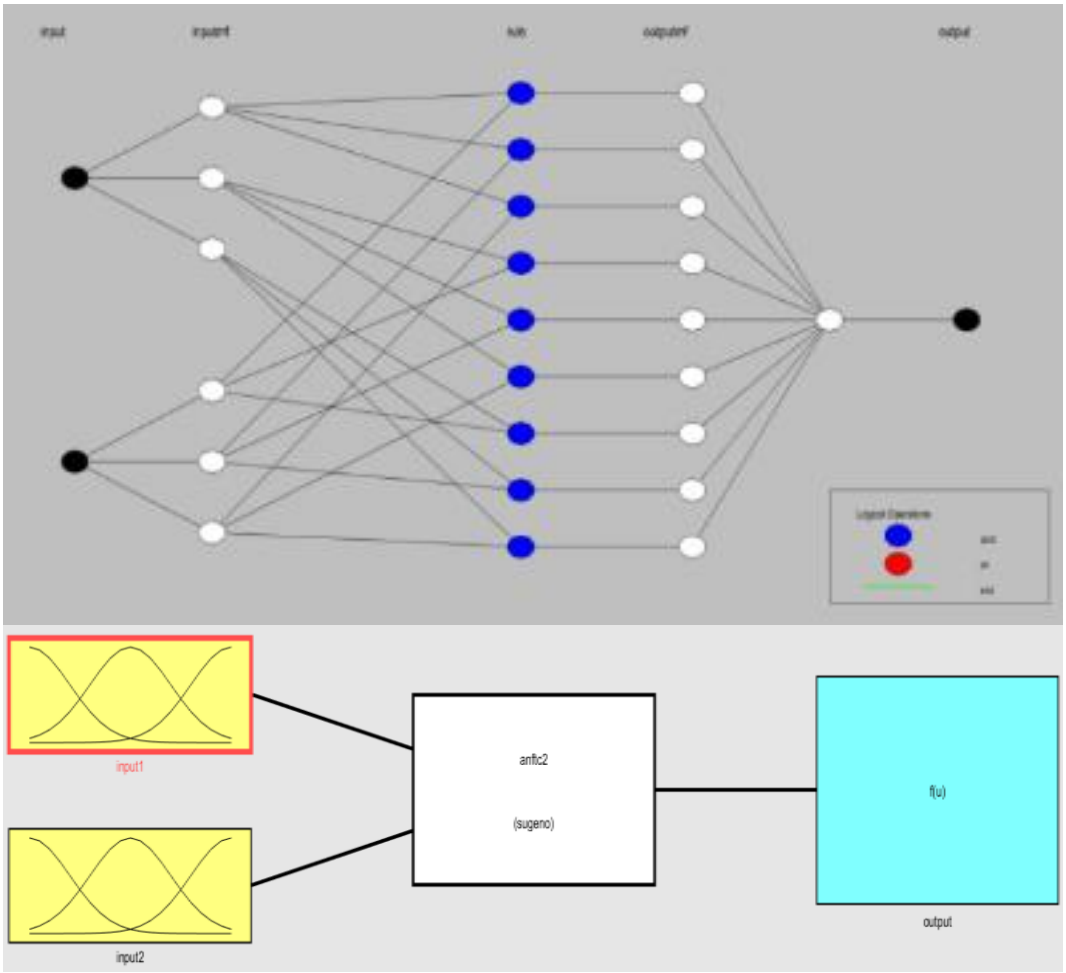

Fig. 6. ANFIS network model (left plot) and ANFIS-FTC method (right plot)

5. Simulation Results

To evaluate the effectiveness of ANFIS-FTC strategy, the closed-loop system has been simulated, and a fault occurs at t=15s. Various scenarios are presented as variations in rotor speed under both control strategies. All nominal parameters are utilized in the different simulations are listed in Table 5 (see Appendix). In these tests, the motor operates under various traction and deceleration conditions in terms of speed profiles.

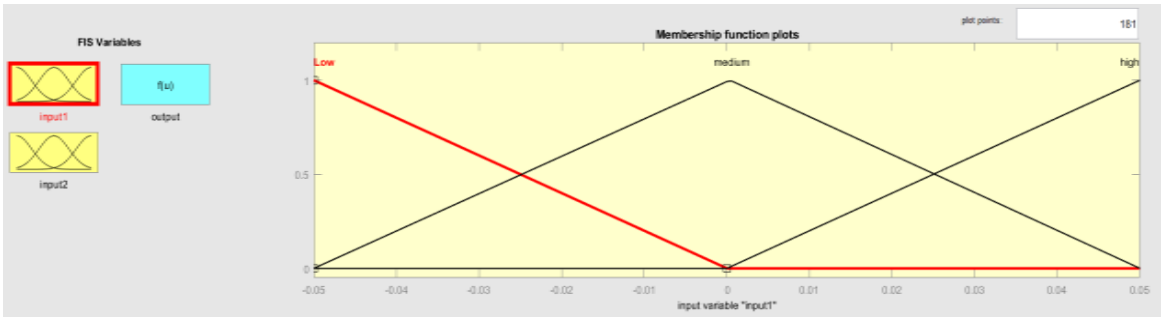

(a)

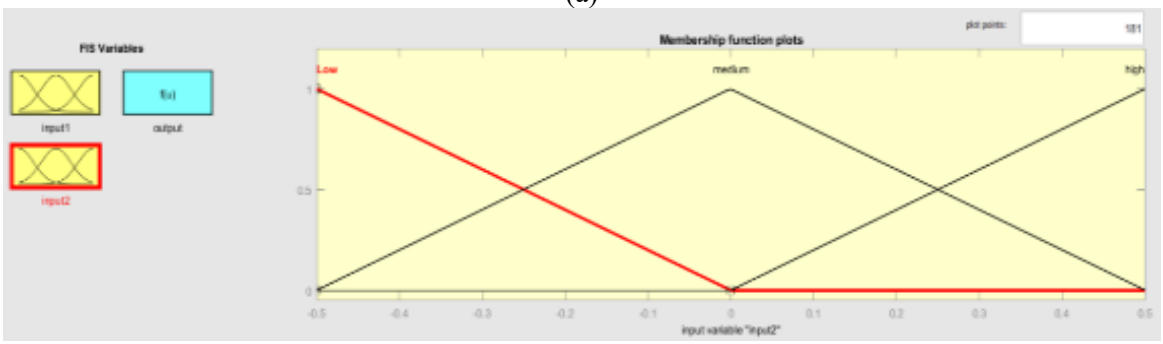

(b)

Fig. 7. The input membership functions: (a) e and (b) Δe

5.1. Performances Test of Conventional FTC

Fig. 8, Fig. 9, Fig. 10 present the obtained results from the conventional FTC algorithm under varying reference speeds and faulty conditions.

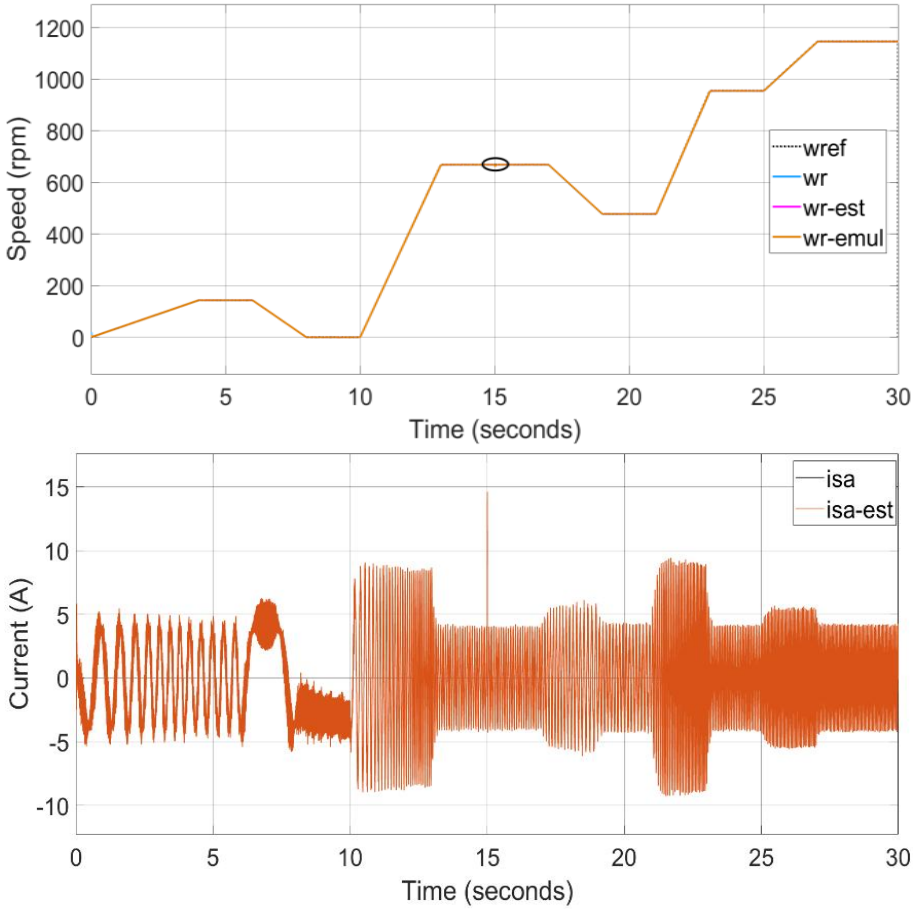

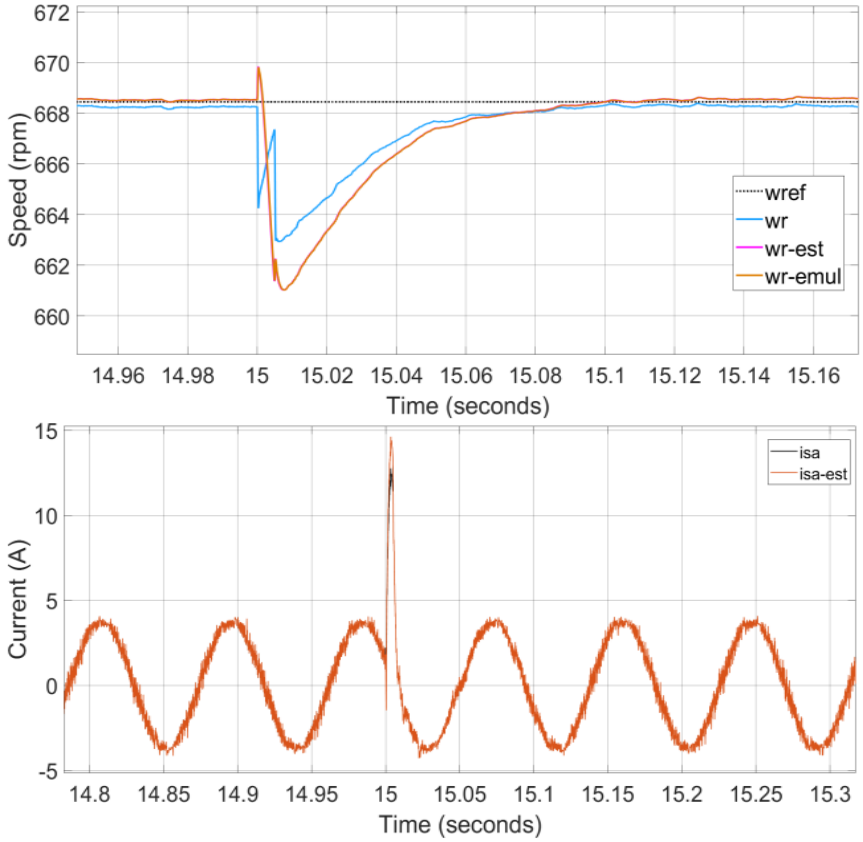

Fig. 8. Reference, the real, estimated, and emulated speeds, along with the stator currents (upper plot) with utilizing conventional FTC and zoomed-in view of the fault occurrence at t=15s (lower plot)

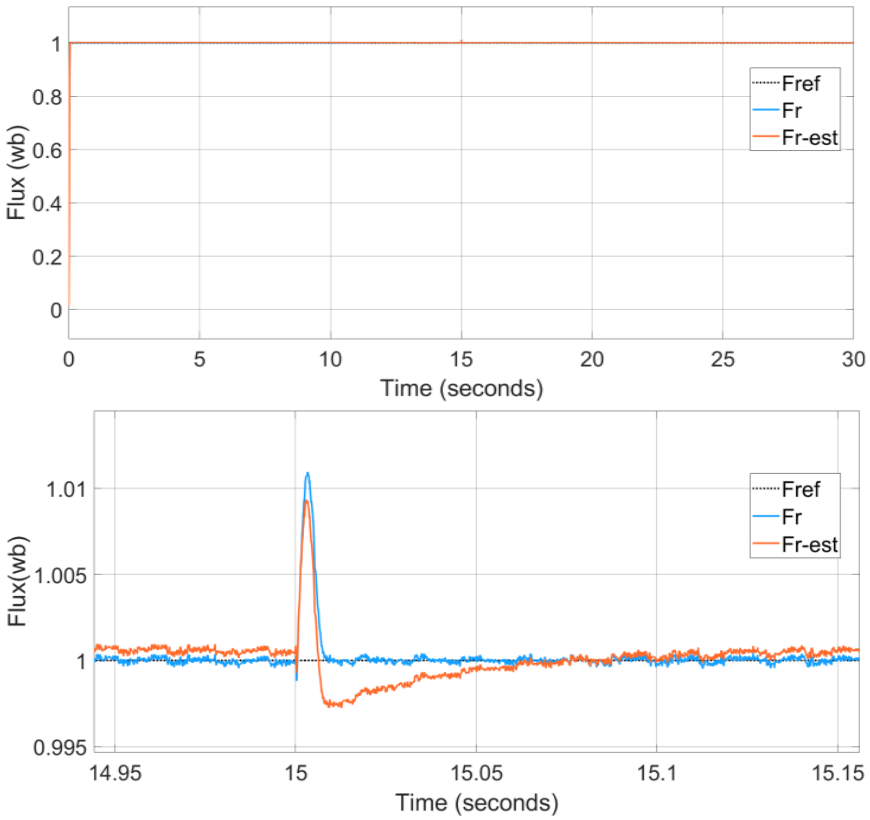

Fig. 9. Reference, the real, and estimated rotor flux (left plot), utilizing conventional FTC and zoomed-in view of the fault occurrence at t=15s (right plot)

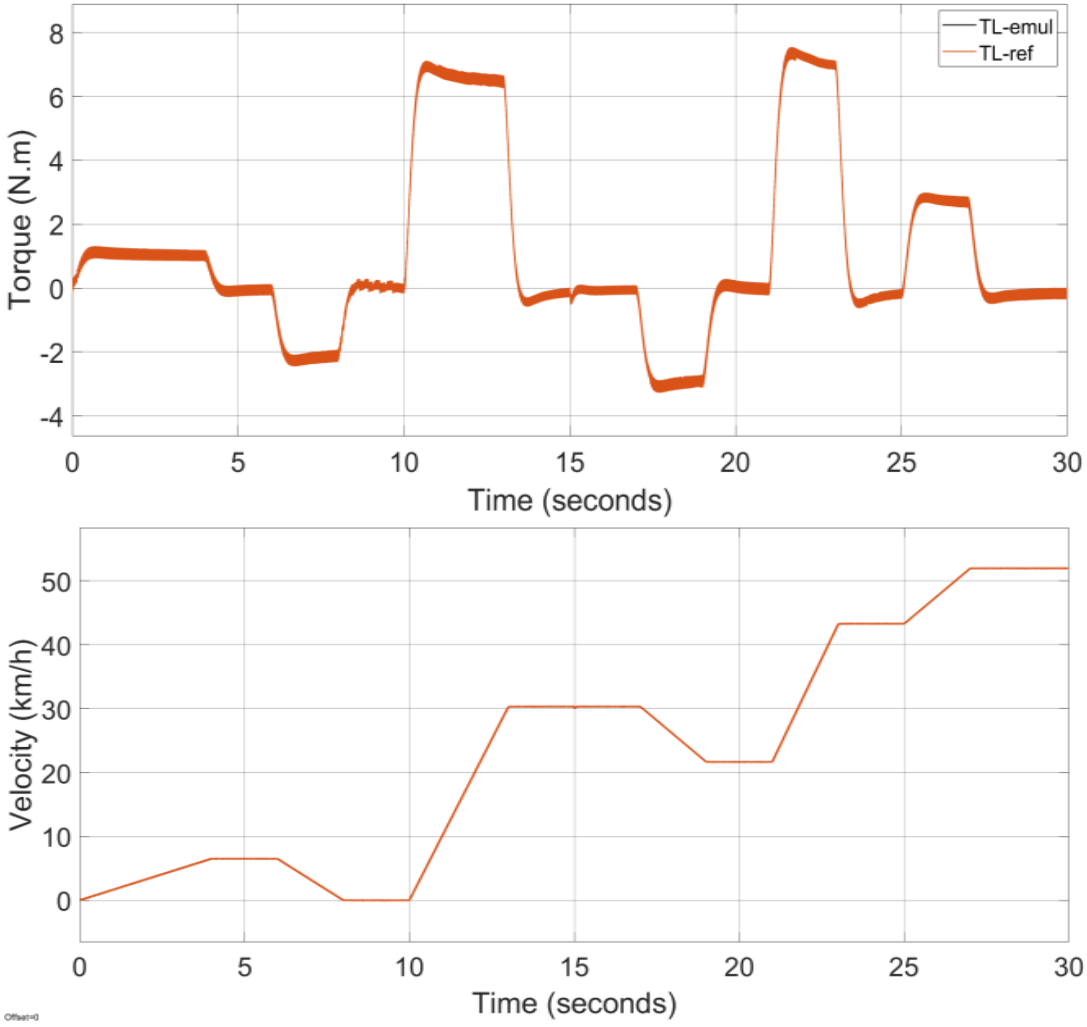

Fig. 10. Reference and emulated torque (left plot), along with the linear speed of EV (right plot), using conventional FTC

Fig. 8, Fig. 9, Fig. 10 show the speed, waveforms of the phase currents, rotor flux, and torque with EV linear speed from healthy to fault-tolerant operations using the conventional FTC. We can see a slight fluctuations when fault occurs at t=15, it soon becomes stable and gradually approaches the reference value.

5.2. Performances Test of ANFIS-FTC

In this case, we have tested the performance of the suggested scheme, which is based on the ANFIS strategy, under the same conditions mentioned in the previous control. Fig. 11, Fig. 12, Fig. 13 illustrate the simulation results of the proposed scheme. As can be seen from these Figures, the estimated fault can be quickly and accurately identified. These results demonstrate the high accuracy of this method in estimating faults. It shows better robustness against faults, requires less recovery time and provides better response.

As evidenced in the obtained results, the proposed algorithm performs effectively under the test conditions, and they indicate that the performance of ANFIS-FTC in faulty conditions presents a significant advantage over conventional FTC. This advantage reduces the impact of faults, enhances performance machine, and ultimately leads to improved efficiency.

In these figures, it is evident that the speeds, flux, stator currents, and torques align with their respective references for both control systems. Consequently, the conventional FTC demonstrates slight fluctuations when faults are introduced. However, it takes more recovery time compared to the ANFIS-FTC.

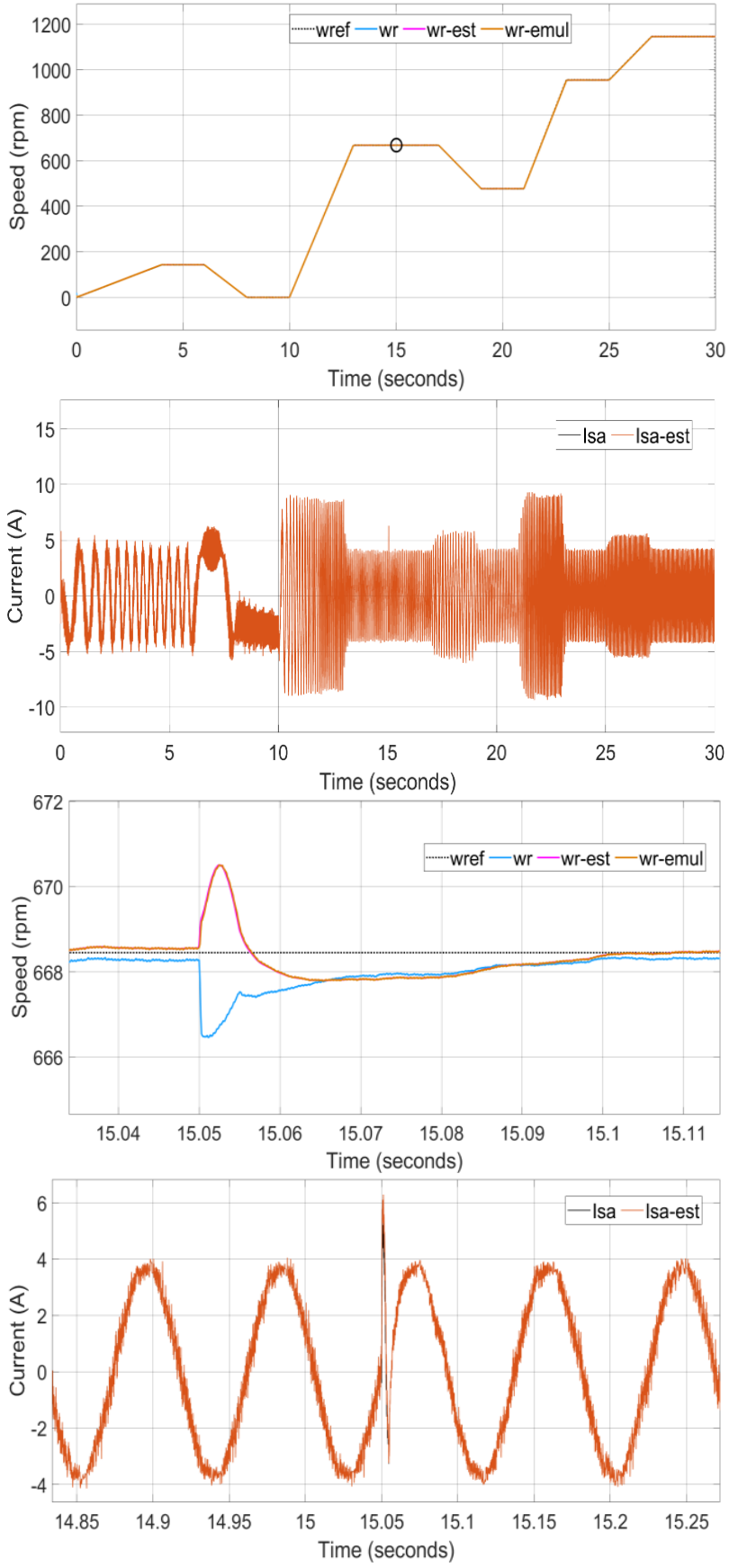

Fig. 11. Reference, the real, estimated, and emulated speeds, along with the stator currents (upper plot) Utilizing ANFIS-FTC and zoomed-in view of the fault occurrence time (lower plot)

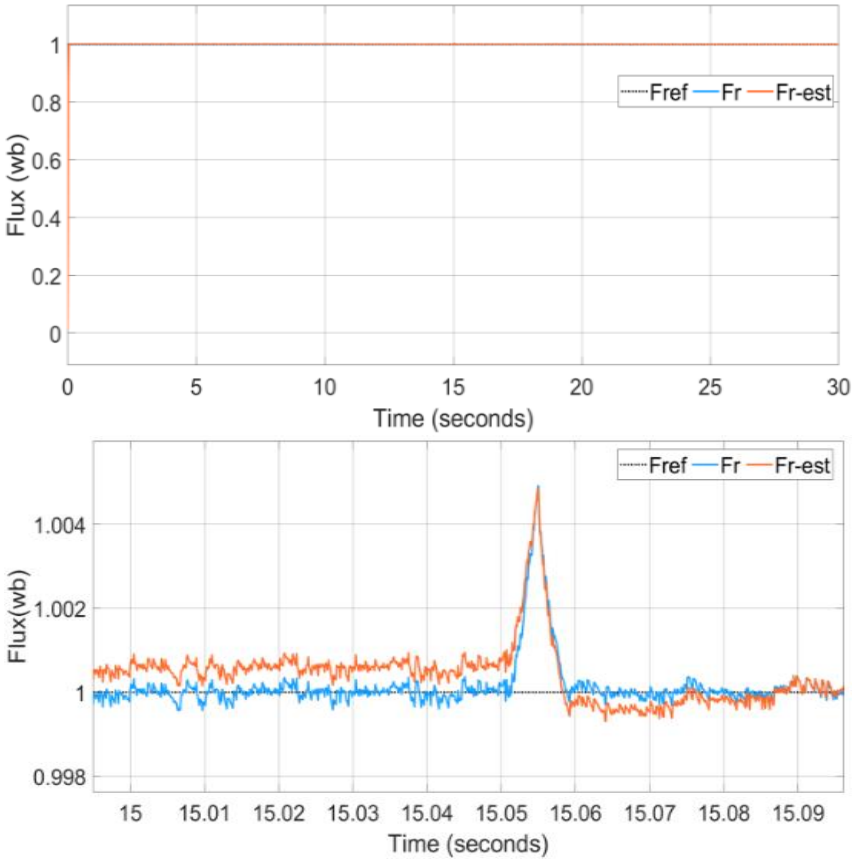

Fig. 12. Reference, the real, and estimated rotor flux (left plot), utilizing ANFIS-FTC and zoomed-in view of the fault occurrence time (right plot)

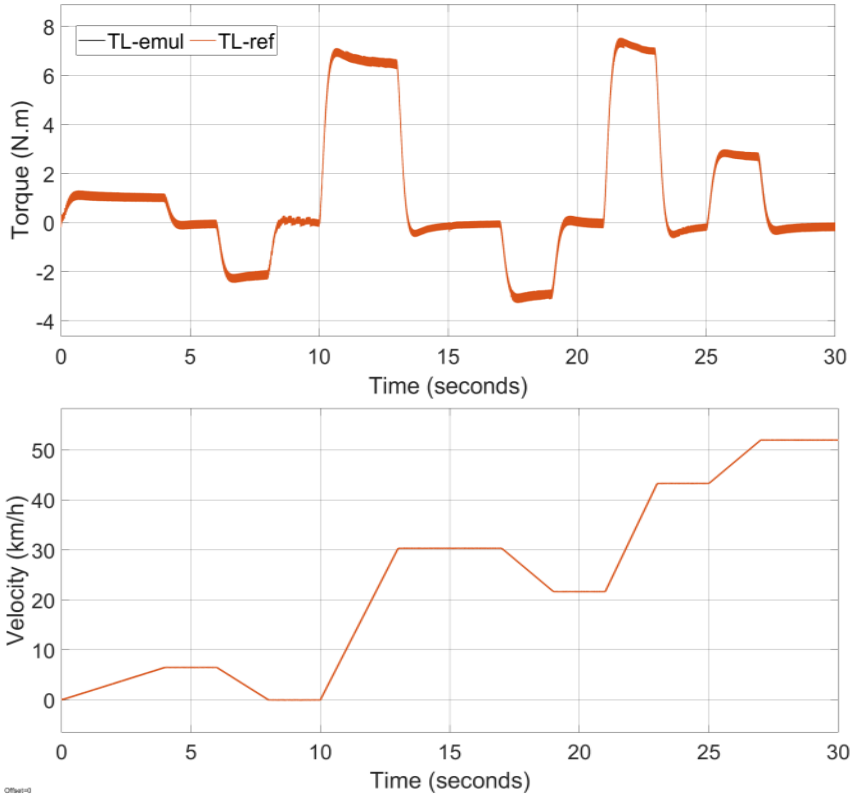

Fig. 13. Reference and emulated torque (left plot), along with the linear speed of EV (right plot), using ANFIS-FTC

5.3. Comparative Study Between ANFIS-FTC and FTC

To highlight the performance of the suggested solution concerning overshoot, fault estimation time, and accuracy, we have focused on comparing the performance of these two control methods. To illustrate a quantitative comparison, the RMSE, IAE, and ISE are calculated and recorded in Table 3.

Table 3. Performances analysis of FTC and ANFIS-FTC

Performances	FTC	ANFIS-FTC	Improvements %
RMSE	0.0737	0.0049	93.35
IAE	0.0400	0.0016	96
ISE	0.0551	0.0012	97.82

Table 4 summarizes the performance metrics of the ANFIS-FTC controller with various controllers available in the literature.

Table 4. Qualitative comparison between the suggested method and recent control strategies

Control Scheme	Fault Tolerance Response (sec)	Accuracy	Overshoot %
Suggested method	0.05 s	high	0.02244
LPV/H_∞-FTC [21]	0.07 s	high	0.02808
AFs-FTC [23]	0.1 s	medium	0.09782
DB-DTFC [25]	0.05 s	high	0.05360
AFTC [36]	0.1 s	medium	0.06125
AANFIS [39]	0.05 s	high	0.02
Fuzzy-FTC [44]	0.2 s	high	0

As shown in Table 4, the suggested controller significantly outperforms the traditional FTCs based on the comparison criteria, particularly in terms of performance measures related to fault tolerance response.

6. Conclusion

This research paper suggested an intelligent FTC based on a neuro-fuzzy approach for a double fed asynchronous motor performance enhancement. This technique is built on the Lunenberger observer and ANFIS models. The proposed control is designed by combining the LO and ANFIS outputs, that the outcome of ANFIS is FTC of DFAM drive. The ANFIS-FTC method has been compared with the conventional FTC for EV application. The obtained results proved that the FTC-based ANFIS setup performed well, demonstrating stable output and an improved response to faults. The performance metrics returned an acceptable value, with a root mean square error of 0.0049.

The superiority of the proposed approach for fault estimation time, overshoot, and accuracy is shown in simulation results. The inclusion of a neuro-fuzzy system into a closed-loop system automates the fault estimation process, reduces the risk of serious failures, and enhances EV operation efficiency. In conclusion, the results of this study offer significant insights for researchers and engineers aiming to improve the performance of FTCs strategies.

Author Contribution: All authors contributed equally to the main contributor to this paper. All authors read and approved the final paper.

Funding: This research received no external funding.

Conflicts of Interest: The authors declare no conflict of interest.

Appendix

Table 5. DFAM nominal parameters

Element	Value
Nominal power (KW)	1.5
Rr (Ω)	3.805
Rs (Ω)	4.85
Lr /Ls (H)	0.274
Lm (H)	0.258
Jm (kg.m^2)	0.031

References

[1] B. Zhang, S. Lu, W. Wu, C. Li and J. Lu, "Robust fault-tolerant control for four-wheel individually actuated electric vehicle considering driver steering characteristics," *Journal of the Franklin Institute*, vol. 358, no. 11, pp. 5883-5908, 2021, https://doi.org/10.1016/j.jfranklin.2021.05.034.

[2] O. Ammari, K. El Majdoub, F. Giri, R. Baz, "Dynamic modelling of the longitudinal movement of an electric vehicle in propulsion mode equipped with BLDC in-wheel motors, taking tire dynamics into account," *IFAC-PapersOnLine*, vol. 58, no. 13, pp. 709-714, 2024, https://doi.org/10.1016/j.ifacol.2024.07.565.

[3] S. Madichetty, S. Mishra, M. Basu, "New trends in electric motors and selection for electric vehicle propulsion systems," *IET Electrical Systems in Transportation,* vol. 11, no. 3, pp. 186-199, 2021, https://doi.org/10.1049/els2.12018.

[4] A. D. Gerlando *et al.*, "Circularity potential of electric motors in e-mobility: methods, technologies, challenges," *Journal of Remanufacturing,* vol. 14, pp. 315–357, 2024, https://doi.org/10.1007/s13243-024-00143-6.

[5] R. Shenbagalakshmi, S.K. Mittal, J. Subramaniyan, V. Vengatesan, D. Manikandan, K. Ramaswamy, "Adaptive speed control of BLDC motors for enhanced electric vehicle performance using fuzzy logic," *Scientific Reports,* vol. 15, p. 12579, 2025, https://doi.org/10.1038/s41598-025-90957-6.

[6] A. Kasri, K. Ouari, Y. Belkhier, M. Bajaj, L. Zaitsev, "Optimizing electric vehicle powertrains peak performance with robust predictive direct torque control of induction motors: a practical approach and experimental validation," *Scientific Reports,* vol. 14, p. 14977, 2024, https://doi.org/10.1038/s41598-024-65988-0.

[7] Z. Sakhri *et al*., "Soft computing approaches of direct torque control for DFIM Motor's," *Cleaner Engineering and Technology*, vol. 24, p. 100891, 2025, https://doi.org/10.1016/j.clet.2025.100891.

[8] L. Al Quraan and L. Számel, "Torque ripple reduction of switched reluctance motor using direct instantaneous torque control and adaptive turn-on technique for electric vehicle applications," *IET Electric Power Applications*, vol. 17, no. 12, pp. 1502-1514, 2023, https://doi.org/10.1049/elp2.12358.

[9] N. Ali and Q. Gao, "Simple current sensor fault-tolerant control strategy for switched reluctance motors in high-reliability applications," *IET Electric Power Applications*, vol. 15, pp. 963-977, 2021, https://doi.org/10.1049/elp2.12058.

[10] S. Mahfoud, N. El Ouanjli, A. Derouich, A. El Idrissi, A. Hilali, E. Chetouani, "Higher performance enhancement of direct torque control by using artificial neural networks for doubly fed induction motor," *e-Prime - Advances in Electrical Engineering, Electronics and Energy*, vol. 8, p. 100537, 2024, https://doi.org/10.1016/j.prime.2024.100537.

[11] Y. Han, "Sensorless Control of Doubly Fed Induction Machines Using Only Rotor-Side Variables," *Symmetry,* vol. 17, no. 5, p. 712, 2025, https://doi.org/10.3390/sym17050712.

[12] A. Chantoufi *et al*., "Direct Torque Control-Based Backstepping Speed Controller of Doubly Fed Induction Motors in Electric Vehicles: Experimental Validation," *IEEE Access*, vol. 12, pp. 139758-139772, 2024, https://doi.org/10.1109/ACCESS.2024.3462821.

[13] A. Chantoufi, A. Derouich, N. El Ouanjli, S. Mahfoud, A. El Idrissi, "Improved direct torque control of doubly fed induction motor in electric vehicles using fuzzy logic controllers," *e-Prime - Advances in Electrical Engineering, Electronics and Energy*, vol. 11, p. 100882, 2025, https://doi.org/10.1016/j.prime.2024.100882.

[14] K. Ni, C. Gan, G. Peng, H. Shi, Y. Hu, and R. Qu, "Power Compensation-Oriented SVM-DPC Strategy for a Fault-Tolerant Back-to-Back Power Converter Based DFIM Shipboard Propulsion System," *IEEE Transactions on Industrial Electronics*, vol. 69, no. 9, pp. 8716–8726, 2022, https://doi.org/10.1109/TIE.2021.3114727.

[15] M. Zerzeri, A. Khedher, "Optimal speed–torque control of doubly-fed induction motors: Analytical and graphical analysis," *Computers & Electrical Engineering*, vol. 93, p. 107258, 2021, https://doi.org/10.1016/j.compeleceng.2021.107258.

[16] M. Pathmanathan, C.C.D. Viana, S. Semsar, and P.W. Lehn, "Open-phase fault tolerant driving operation of dual-inverter-based traction drive," *IET Electric Power Applications*, vol. 15, no. 7, pp. 873-889, 2021, https://doi.org/10.1049/elp2.12067.

[17] C. P. Gor, V. A. Shah, and B. Rangachar, "Fuzzy logic based dynamic performance enhancement of five phase induction motor under arbitrary open phase fault for electric vehicle," *International Journal of Emerging Electric Power Systems*, vol. 22, no. 4, pp. 473-492, 2021, https://doi.org/10.1515/ijeeps-2020-0271.

[18] L. Gang, G. Pingshu, L. Junjie, Z. Tao, C. Yanli, L. Xiaobei, "Fault Tolerant Control for Distributed Drive Electric Vehicle Based on Co-simulation of Carsim and Matlab," *IFAC-PapersOnLine*, vol. 54, no. 10, pp. 514-519, 2021, https://doi.org/10.1016/j.ifacol.2021.10.214.

[19] V.A. Racanelli, S. Mascolo, "Safe and Fault Tolerant Control of Industrial differential Drive Vehicles," *IFAC-PapersOnLine*, vol. 58, no. 4, pp. 150-155, 2024, https://doi.org/10.1016/j.ifacol.2024.07.209.

[20] X. Li, P. Ge, T. Zhang, Y. Wang, J. Liu, F. Cui, "Fault Tolerant Control Method of Distributed Drive Electric Vehicles Based on Observer," *IFAC-PapersOnLine*, vol. 58, no. 29, pp. 94-99, 2024, https://doi.org/10.1016/j.ifacol.2024.11.126.

[21] X. Cao, Y. Tian, X. Ji and B. Qiu, "Fault-Tolerant Controller Design for Path Following of the Autonomous Vehicle Under the Faults in Braking Actuators," *IEEE Transactions on Transportation Electrification*, vol. 7, no. 4, pp. 2530-2540, 2021, https://doi.org/10.1109/TTE.2021.3071725.

[22] M. Hamouda *et al*., "A Novel Interturn Fault Tolerant-Based Average Torque Control of Switched Reluctance Motors for Electric Vehicles," *IEEE Access*, vol. 12, pp. 111769-111781, 2024, https://doi.org/10.1109/ACCESS.2024.3406488.

[23] L. Cai and J. Yang, "Asymptotic Stability of Electric-Vehicle-to-Grid System With Actuator Faults," *IEEE Transactions on Transportation Electrification*, vol. 7, no. 4, pp. 2439-2452, 2021, https://doi.org/10.1109/TTE.2021.3068455.

[24] R. Tabasian, M. Ghanbari, A. Esmaeli, & M. Jannati, "A novel direct field-oriented control strategy for fault-tolerant control of induction machine drives based on EKF," *IET Electric Power Applications*, vol. 15, no. 8, pp. 979-997, 2021, https://doi.org/10.1049/elp2.12051.

[25] Z. Liu, H. Zhou, Z. Zhou, & G. Liu, "Torque dynamic performance enhancement of five-phase permanent magnet synchronous motor with open-circuit fault," *IET Electric Power Applications*, vol. 18, no. 11, pp. 1530-1539, 2024, https://doi.org/10.1049/elp2.12513.

[26] H. Deng, Y. Zhao, A. T. Nguyen, and C. Huang, "Fault-Tolerant Predictive Control With Deep-Reinforcement-Learning-Based Torque Distribution for Four In-Wheel Motor Drive Electric Vehicles," *IEEE/ASME Transactions on Mechatronics*, vol. 28, no. 2, pp. 668-680, 2023, https://doi.org/10.1109/TMECH.2022.3233705.

[27] H. Park, T. Kim and Y. Suh, "Fault-Tolerant Control Methods for Reduced Torque Ripple of Multiphase BLDC Motor Drive System Under Open-Circuit Faults," *IEEE Transactions on Industry Applications*, vol. 58, no. 6, pp. 7275-7285, 2022, https://doi.org/10.1109/TIA.2022.3191633.

[28] A. Moussaoui, D. Ben Attous, H. Benbouhenni, Y. Bekakra, B. Nedjadi, Z.M.S. Elbarbary, "Enhanced direct torque control based on intelligent approach for doubly-fed induction machine fed by three-level inverter," *Heliyon*, vol. 10, no. 21, p. e39738, 2024, https://doi.org/10.1016/j.heliyon.2024.e39738.

[29] E. Pérez-Pérez, V. Puig, F. López-Estrada, G. Valencia-Palomo, I. Santos-Ruiz, "Neuro-fuzzy Takagi Sugeno observer for fault diagnosis in wind turbines," *IFAC-PapersOnLine*, vol. 56, no. 2, pp. 3522-3527, 2023, https://doi.org/10.1016/j.ifacol.2023.10.1508.

[30] N. Basil and H. M. Marhoon, "Selection and evaluation of FOPID criteria for the X-15 adaptive flight control system (AFCS) via Lyapunov candidates: Optimizing trade-offs and critical values using optimization algorithms," *e-Prime – Advances in Electrical Engineering, Electronics and Energy*, vol. 6, p. 100305, 2023, https://doi.org/10.1016/j.prime.2023.100305.

[31] N. Basil, H.M. Marhoon, "Correction to: selection and evaluation of FOPID criteria for the X-15 adaptive flight control system (AFCS) via Lyapunov candidates: Optimizing trade-offs and critical values using optimization algorithms," *e-Prime - Advances in Electrical Engineering, Electronics and Energy*, vol. 8, p. 100589, 2024, https://doi.org/10.1016/j.prime.2024.100589.

[32] N. Basil *et al*., "Performance analysis of hybrid optimization approach for UAV path planning control using FOPID-TID controller and HAOAROA algorithm," *Scientific Reports*, vol. 15, no. 1, p. 4840, 2025, https://doi.org/10.1038/s41598-025-86803-4.

[33] A. F. Mohammed, H. M. Marhoon, N. Basil, and A. Ma'arif, "A new hybrid intelligent fractional order proportional double derivative + integral (FOPDD+I) controller with ANFIS simulated on automatic voltage regulator system," *International Journal of Robotics & Control Systems*, vol. 4, no. 2, pp. 463-479, 2024, https://doi.org/10.31763/ijrcs.v4i2.1336.

[34] N. Basil, H. M. Marhoon, and A. F. Mohammed, "Evaluation of a 3-DOF helicopter dynamic control model using FOPID controller-based three optimization algorithms," *International Journal of Information Technology*, pp. 1–10, 2024, https://doi.org/10.1007/s41870-024-02373-0.

[35] N. Basil, B. M. Sabbar, H. M. Marhoon, A. F. Mohammed, and A. Ma'arif, "Systematic review of unmanned aerial vehicles control: Challenges, solutions, and meta-heuristic optimization," *International Journal of Robotics & Control Systems*, vol. 4, no. 4, pp. 1794-1818, 2024, https://doi.org/10.31763/ijrcs.v4i4.1596.

[36] T. Roubache and S. Chaouch, "Nonlinear Fault Tolerant Control of Dual Three-Phase Induction Machines based Electric Vehicles," *Revue Roumaine des Sciences Techniques — Série Électrotechnique Et Énergétique*, vol. 68, no. 1, pp. 65–70, 2023, https://doi.org/10.59277/RRST-EE.2023.68.1.11.

[37] J. Teng, C. Li, Y. Feng, T. Yang, R. Zhou, and Q. Z. Sheng, "Adaptive observer based fault tolerant control for sensor and actuator faults in wind turbines," *Sensors*, vol. 21, no. 24, p. 8170, 2021, https://doi.org/10.3390/s21248170.

[38] Q. Jia, L. Wu, and H. Li, "Robust actuator fault reconstruction for Takagi-Sugeno fuzzy systems with time-varying delays via a synthesized learning and Luenberger observer," *International Journal of Control, Automation and Systems*, vol. 9, no. 2, pp. 799-809, 2021, https://doi.org/10.1007/s12555-019-0747-4.

[39] K. V. S. H. G. Sarman, T. Madhu, and A. M. Prasad, "Fault diagnosis of BLDC drive using advanced adaptive network-based fuzzy inference system," *Soft Computing*, vol. 25, no. 20, pp. 12759–12774, 2021, https://doi.org/10.1007/s00500-021-06046-z.

[40] E. Pérez-Pérez, J. Fragoso-Mandujano, J. Guzmán-Rabasa, Y. González-Baldizón, S. Flores-Guirao, "ANFIS and Takagi–Sugeno interval observers for fault diagnosis in bioprocess system," *Journal of Process Control*, vol. 138, p. 103225, 2024, https://doi.org/10.1016/j.jprocont.2024.103225.

[41] T. Thanaraj, K. H. Low, and B. F. Ng, "Actuator fault detection and isolation on multi-rotor UAV using extreme learning neuro-fuzzy systems," *ISA transactions*, vol. 138, pp. 168-185, 2023, https://doi.org/10.1016/j.isatra.2023.02.026.

[42] Z. Zemali *et al*., "Robust intelligent fault diagnosis strategy using Kalman observers and neuro-fuzzy systems for a wind turbine benchmark," *Renewable Energy*, vol. 205, pp. 873-898, 2023, https://doi.org/10.1016/j.renene.2023.01.095.

[43] M. Pathmanathan, S. Semsar, C. Viana and P. W. Lehn, "Power Sharing Control Algorithm for Direct Integration of Fuel Cells in a Dual-Inverter Electric Vehicle Drivetrain," *IEEE Transactions on Transportation Electrification*, vol. 8, no. 2, pp. 2490-2500, 2022, https://doi.org/10.1109/TTE.2022.3143092.

[44] G. Kulandaivel, E. Sundaram, M. Gunasekaran, and S. Chenniappan, "Five-phase induction motor drive-a comprehensive review," *Frontiers in Energy Research*, vol. 11, p. 1178169, 2023, https://doi.org/10.3389/fenrg.2023.1178169.

[45] J. El-bakkouri, H. Ouadi, A. Saad, "Adaptive Neuro Fuzzy Inference System Based controller for Electric Vehicle's hybrid ABS braking," *IFAC-PapersOnLine*, vol. 55, no. 12, pp. 371-376, 2022, https://doi.org/10.1016/j.ifacol.2022.07.340.

[46] C. Liu, K. T. Chau, C. H. Lee, and Z. Song, "A critical review of advanced electric machines and control strategies for electric vehicles," *Proceedings of the IEEE,* vol. 109, no. 6, pp. 1004-1028, 2021, https://doi.org/10.1109/JPROC.2020.3041417.

[47] M. Subbarao, K. Dasari, S. S. Duvvuri, K. R. K. V. Prasad, B. K. Narendra, and V. M. Krishna, "Design, control and performance comparison of PI and ANFIS controllers for BLDC motor driven electric vehicles," *Measurement: Sensors*, vol. 31, p. 101001, 2024, https://doi.org/10.1016/j.measen.2023.101001.

[48] T. Roubache, S. Chaouch, "ANFIS Controller MPPT Algorithm for Solar powered Dual Three Phase Induction Motor based EVs," *Przeglad Elektrotechniczny*, vol. 24, no. 3, 269-274, 2024, https://pe.org.pl/articles/2024/3/47.pdf.

[49] I. Sami, S. Ullah, L. Khan, A. Al-Durra, and J. S. Ro, "Integer and fractional-order sliding mode control schemes in wind energy conversion systems: Comprehensive review, comparison, and technical insight," *Fractal and Fractional*, vol. 6, no. 8, p. 447, 2022, https://doi.org/10.3390/fractalfract6080447.

[50] M. Karahan, M. Inal, C. Kasnakoglu, "Fault Tolerant Super Twisting Sliding Mode Control of a Quadrotor UAV Using Control Allocation," *International Journal of Robotics and Control Systems*, vol. 3, no. 2, pp. 270-285, 2023, https://doi.org/10.31763/ijrcs.v3i2.994.

[51] I. Sami, S. Ullah, S. U. Amin, A. Al-Durra, N. Ullah, and J. Ro, "Convergence Enhancement of Super-Twisting Sliding Mode Control Using Artificial Neural Network for DFIG-Based Wind Energy Conversion Systems," *IEEE Access*, vol. 10, pp. 97625-97641, 2022, https://doi.org/10.1109/ACCESS.2022.3205632.

[52] J. Wang, D. Bo, Q. Miao, Z. Li, X. Wu, and D. Lv, "Maximum power point tracking control for a doubly fed induction generator wind energy conversion system based on multivariable adaptive super-twisting approach," *International Journal of Electrical Power & Energy Systems,* vol. 124, p. 106347, 2021, https://doi.org/10.1016/j.ijepes.2020.106347.

[53] K. Shao, J. Zheng, M. Fu, "Review on the developments of sliding function and adaptive gain in sliding mode control," *Journal of Automation and Intelligence*, 2025, https://doi.org/10.1016/j.jai.2025.06.001.

[54] B. Shweta and Dr. V. Sadhana, "Model Predictive Control and Higher Order Sliding Mode Control for Optimized and Robust Control of PMSM," *IFAC-Papers OnLine*, vol. 55, no. 22, pp. 195-200, 2022, https://doi.org/10.1016/j.ifacol.2023.03.033.

[55] J. Li, C. Yang, J. Fang, and Y. Zhang, "A Fault-Tolerant Trajectory Tracking Strategy of Four-Wheel Independent Drive Electric Vehicles Using Super-Twisting Sliding Model Control," *IEEE Transactions on Transportation Electrification*, vol. 11, no. 1, pp. 3907-3917, 2025, https://doi.org/10.1109/TTE.2024.3447761.

[56] D. Castellanos-Cárdenas *et al*., "A Review on Data-Driven Model-Free Sliding Mode Control," *Algorithms,* vol. 17, no. 12, p. 543, 2024, https://doi.org/10.3390/a17120543.

[57] K. Makhloufi, S. Zegnoun, A. Omari, and I. K. Bousserhane, "Adaptive Neuro-Fuzzy-Slip Control of A Linear Synchronous Machine," *Revue Roumaine Des Sciences Techniques — Série Électrotechnique Et Énergétique*, vol. 67, no. 4, pp. 425-431, 2022, https://journal.iem.pub.ro/rrst-ee/article/view/255.

[58] A. Ounissi, A. Kaddouri, M.S. Aggoun, and R. Abdessemed, "Second Order Sliding Mode Controllers of Micropositioning Stage Piezoelectric Actuator With Colman-Hodgdon Model Parameters," *Revue Roumaine Des Sciences Techniques — Série Électrotechnique Et Énergétique*, vol. 67, no. 1, pp. 41-46, 2022, https://journal.iem.pub.ro/rrst-ee/article/view/153.

[59] N. Z. Laabidine, B. Bossoufi, I. El Kafazi, C. El Bekkali, and N. El Ouanjli, "Robust Adaptive Super Twisting Algorithm Sliding Mode Control of a Wind System Based on the PMSG Generator," *Sustainability,* vol. 15, no. 14, p. 10792, 2023, https://doi.org/10.3390/su151410792.

[60] H. Xiao, Z. Zhen, and Y. Xue, "Fault-tolerant attitude tracking control for carrier-based aircraft using RBFNN-based adaptive second-order sliding mode control," *Aerospace Science and Technology*, vol. 139, p. 108408, 2023, https://doi.org/10.1016/j.ast.2023.108408.

[61] J. George and G. Mani, "A Portrayal of Sliding Mode Control Through Adaptive Neuro Fuzzy Inference System With Optimization Perspective," *IEEE Access*, vol. 12, pp. 3222-3239, 2024, https://doi.org/10.1109/ACCESS.2023.3348836.

[62] P. Mahesh and S. R. Arya, "Randomized Self-Structuring Adaptive Neuro-Fuzzy Based Induction Motor Drives with Optimized FOPI Gains," *CPSS Transactions on Power Electronics and Applications*, vol. 9, no. 4, pp. 465-475, 2024, https://doi.org/10.24295/CPSSTPEA.2024.00026.

[63] J. Wang, Y. Gao, Y. Cao, and T. Tang, "The Investigation of Data Voting Algorithm for Train Air-Braking System Based on Multi-Classification SVM and ANFIS," *Chinese Journal of Electronics*, vol. 33, no. 1, pp. 274-281, 2024, https://doi.org/10.23919/cje.2021.00.428.

[64] S. Kanwal and S. Jiriwibhakorn, "Advanced Fault Detection, Classification, and Localization in Transmission Lines: A Comparative Study of ANFIS, Neural Networks, and Hybrid Methods," *IEEE Access*, vol. 12, pp. 49017-49033, 2024, https://doi.org/10.1109/ACCESS.2024.3384761.

[65] M. Elsisi, M. Tran, K. Mahmoud, M. Lehtonen and M. M. F. Darwish, "Robust Design of ANFIS-Based Blade Pitch Controller for Wind Energy Conversion Systems Against Wind Speed Fluctuations," *IEEE Access*, vol. 9, pp. 37894-37904, 2021, https://doi.org/10.1109/ACCESS.2021.3063053.

[66] S. Samantaray, P. Sahoo, A. Sahoo, and D. P. Satapathy, "Flood discharge prediction using improved ANFIS model combined with hybrid particle swarm optimisation and slime mould algorithm," *Environmental Science and Pollution Research*, vol. 30, no. 35, pp. 83845-83872, 2023, https://doi.org/10.1007/s11356-023-27844-y.

[67] R. Patra, P. Chaudhary, and O. Shah, "Design and Development of ANFIS based Controller for Three Phase Grid Connected System," *International Journal of Robotics and Control Systems*, vol. 4, no.1, pp. 125-138, 2024, https://doi.org/10.31763/ijrcs.v4i1.1242.

[68] W. Sultana, S. D. S. Jebaseelan, "ANFIS controller for photovoltaic inverter transient and voltage stability enhancement," *Measurement: Sensors*, vol. 33, p. 101154, 2024, https://doi.org/10.1016/j.measen.2024.101154.

[69] S. O. Sada, S. C. Ikpeseni, "Evaluation of ANN and ANFIS modeling ability in the prediction of AISI 1050 steel machining performance," *Heliyon*, vol. 7, no. 2, p. e06136, 2021, https://doi.org/10.1016/j.heliyon.2021.e06136.

[70] I. Govindharaj *et al.*, "Sensorless vector-controlled induction motor drives: Boosting performance with Adaptive Neuro-Fuzzy Inference System integrated augmented Model Reference Adaptive System," *MethodsX*, vol. 13, p. 102992, 2024, https://doi.org/10.1016/j.mex.2024.102992.

[71] J. B. Banu, J. Jeyashanthi, and A. T. Ansari, "DTC-IM drive using adaptive neuro fuzzy inference strategy with multilevel inverter," *Journal of Ambient Intelligence and Humanized Computing*, vol. 13, pp. 4799-4821, 2022, https://doi.org/10.1007/s12652-021-03244-3.

[72] V. D. Sagias, P. Zacharia, A. Tempeloudis, C. Stergiou, "Adaptive Neuro-Fuzzy Inference System-Based Predictive Modeling of Mechanical Properties in Additive Manufacturing," *Machines*, vol. 12, no. 8, p. 523, 2024, https://doi.org/10.3390/machines12080523.

[73] G. Dyanamina and S. K. Kakodia, "Adaptive neuro fuzzy inference system based decoupled control for neutral point clamped multi level inverter fed induction motor drive," *Chinese Journal of Electrical Engineering*, vol. 7, no. 2, pp. 70-82, 2021, https://doi.org/10.23919/CJEE.2021.000017.

[74] L. Dubchak *et al.*, "Adaptive Neuro-Fuzzy System for Detection of Wind Turbine Blade Defects," *Energies*, vol. 17, no. 24, p. 6456, 2024, https://doi.org/10.3390/en17246456.

[75] S. Ouhssain, H. Chojaa, Y. Aljarhizi, E. Al Ibrahmi, A. Maarif, and M. A. Mossa, "Enhancing the Performance of a Wind Turbine Based DFIG Generation System Using an Effective ANFIS Control Technique," *International Journal of Robotics and Control Systems*, vol. 4, no. 4, p. pp. 1617-1640, 2024, https://doi.org/10.31763/ijrcs.v4i4.1451.

[76] K. Choi and H. Chang, "Improvement of Adaptive Cruise Control System Performance on Sloped Roads Based on Adaptive Neuro-Fuzzy Inference System," *IEEE Access*, vol. 13, pp. 60519-60531, 2025, https://doi.org/10.1109/ACCESS.2025.3557089.

[77] M. A. George, D. V. Kamat, C. P. Kurian, "Electric vehicle speed tracking control using an ANFIS-based fractional order PID controller," *Journal of King Saud University - Engineering Sciences*, vol. 36, no. 4, pp. 256-264, 2024, https://doi.org/10.1016/j.jksues.2022.01.001.

[78] M. S. Rahman, and M. H. Ali, "Adaptive Neuro Fuzzy Inference System (ANFIS)-Based Control for Solving the Misalignment Problem in Vehicle-to-Vehicle Dynamic Wireless Charging Systems," *Electronics*, vol. 14, no. 3, p. 507, 2025, https://doi.org/10.3390/electronics14030507.

[79] M. K. Oudah, S. W. Shneen, S. A. Aessa, "Reduction of Large Scale Linear Dynamic MIMO Systems Using Adaptive Network Based Fuzzy Inference System," *International Journal of Robotics and Control Systems*, vol. 5, no. 2, pp. 678-697, 2025, https://doi.org/10.31763/ijrcs.v5i2.1684.

[80] M. A. George, D. V. Kamat and C. P. Kurian, "Electronically Tunable ACO Based Fuzzy FOPID Controller for Effective Speed Control of Electric Vehicle," *IEEE Access*, vol. 9, pp. 73392-73412, 2021, https://doi.org/10.1109/ACCESS.2021.3080086.